Hydrol. Earth Syst. Sci. Discuss., 10, 12537–12571, 2013
www.hydrol-earth-syst-sci-discuss.net/10/12537/2013/
doi:10.5194/hessd-10-12537-2013

Hydrology and Earth System Sciences
Open Access
Discussions

Does consideration of water routing affect simulated water and carbon dynamics in terrestrial ecosystems?

G. Tang[1], E. M. Schneiderman[2], L. E. Band[3], T. Hwang[4], D. C. Pierson[2], S. M. Pradhanang[5], and M. S. Zion[2]

[1]Division of Earth and Ecosystem Sciences, Desert Research Institute, Reno, NV, USA
[2]New York City Department of Environmental Protection, Kingston, NY, USA
[3]Department of Geography, University of North Carolina, Chapel Hill, NC, USA
[4]Institute for the Environment, University of North Carolina, Chapel Hill, NC, USA
[5]Institute for Sustainable Cities, City University of New York, New York, NY, USA

Received: 24 September 2013 – Accepted: 4 October 2013 – Published: 17 October 2013

Correspondence to: G. Tang (tangg2010@gmail.com)

Published by Copernicus Publications on behalf of the European Geosciences Union.

Abstract

The cycling of carbon in terrestrial ecosystems is closely coupled with the cycling of water. An important mechanism connecting ecological and hydrological processes in terrestrial ecosystems is lateral flow of water along landscapes. Few studies, however, have examined explicitly how consideration of water routing affects simulated water and carbon dynamics in terrestrial ecosystems. The objective of this study is to explore how consideration of water routing in a process-based hydroecological model affects simulated water and carbon dynamics. To achieve that end, we rasterized the regional hydroecological simulation systems (RHESSys) and employed the rasterized RHESSys (R-RHESSys) in a forested watershed. We performed and compared two contrasting simulations, one with and another without water routing. We found that R-RHESSys is able to correctly simulate major hydrological and ecological variables regardless of whether water routing is considered. When water routing was neglected, however, soil water table depth and saturation deficit were simulated to be smaller and spatially more homogeneous. As a result, evaporation, forest productivity and soil heterotrophic respiration also were simulated to be spatially more homogeneous compared to simulation with water routing. When averaged for the entire watershed, however, differences in simulated water and carbon fluxes are not significant between the two simulations. Overall, the study demonstrated that consideration of water routing enabled R-RHESSys to better capture our preconception of the spatial patterns of water table depth and saturation deficit across the watershed. Because the spatial pattern of soil moisture is fundamental to water efflux from land to the atmosphere, forest productivity and soil microbial activity, ecosystem and carbon cycle models, therefore, need to explicitly represent water routing in order to accurately quantify the magnitudes and patterns of water and carbon fluxes in terrestrial ecosystems.

HESSD

10, 12537–12571, 2013

1 Introduction

The cycling of carbon in terrestrial ecosystems is closely coupled with the cycling of water. Plants need water to survive, and thus, the distribution, composition and structure of plant communities are directly influenced by the spatial patterns of available water (Asbjornsen et al., 2011; Ivanov et al., 2008). An important mechanism that connects ecological and hydrological processes in terrestrial ecosystems is lateral water flow along landscapes. Lateral water flow can redistribute water and nutrients through space, which affects plant establishment, growth and leaf phenology (Asbjornsen et al., 2011); ecosystem structure and function (Wang et al., 2009); and soil biogeochemical processes, such as organic matter decomposition (Ju et al., 2006; Riveros-Iregui et al., 2011). For example, studies have demonstrated that lateral water flow and connectivity act as important determinants of ecological pattern and process in heterogeneous landscapes (Sponseller and Fisher, 2008), and contribute to changes in surface water, energy, nutrients, and carbon in space (Pockman and Small, 2010). In mountainous catchments, Hwang et al. (2012) found that lateral water flow can produce important patterns in water and nutrient fluxes and stores, which influences the long-term spatial development of forest ecosystems. Riveros-Iregui et al. (2011) suggested that landscape-imposed redistribution of soil water is major causes for distinct variation of growing season soil CO_2 efflux within small subalpine watersheds.

Hydrological connectivity via lateral water flow plays important roles in the transport of water, nutrients and sediments at catchment scales (Smith et al., 2010). Correspondingly, distributed hydrology models (DHM) that simulates lateral water flow and its spatial connectivity along landscapes or among simulated grids have been developed increasingly in recent years (Lane et al., 2009). These models, such as DHSVM (Wigmosta et al., 1994) and RHESSys (Tague and Band, 2004), coupled runoff generation and water routing mechanisms and thus are able to explicitly simulate the effects of topographic and subsurface heterogeneities on downslope redistribution of water and nutrients (Doten et al., 2006). In fact, DHMs are widely used to identify saturated ar-

HESSD
10, 12537–12571, 2013

eas that produce runoff and non-point source pollution (Gerard-Marchanti et al., 2006), evaluate irrigation systems (Singh et al., 2006), and examine flood potential associated with disturbances such as deforestation (Doten et al., 2006). The representation of soil moisture variability and water routing processes at grid cell level in DHMs also enables these models to account for the spatial variability of runoff-generating mechanisms and to infer model parameterization from distributed geospatial data such as geology, topography, soils, and land cover (Wang et al., 2011). These advantages greatly contributed to the accuracy of hydrologic forecasting (Smith et al., 2012).

Despite the fact that lateral water flow redistributes water and nutrients in space and thus affects ecosystem structure and function as well as the cycling of water and carbon, however, the representation of lateral water flow and its spatial connectivity may not be adequate in existing ecosystem and carbon cycle models. For example, Riveros-Iregui et al. (2011) indicated that the robust implementation of the lateral redistribution of soil water into biogeochemical models is often lacking. Chen et al. (2005) argued that most carbon cycle models at regional and global scales use bucket models to estimate soil moisture and ignore lateral exchanges of water among simulated units. The causes for such inadequacy are (i) lack of detailed information on how lateral water flow may affect vegetation, water and carbon dynamics in terrestrial ecosystems, and (ii) increased burden of computing when water routing is considered in the model's simulation (Ju et al., 2006; Zhou et al., 2010). This inadequacy, however, is likely to hinder better quantification of the spatial heterogeneity and complex linkages of hydrological, ecological and biogeochemical processes in terrestrial ecosystems.

Furthermore, mountain forests account for about 23 % of the Earth's forest cover and play an important role in modulating the global cycling of water and carbon (Price et al., 2011). Given the elevational gradient in mountain forests plus gravity, lateral water flow – such as subsurface lateral flow along slopes – is common in humid mountain forests (Ridolfi et al., 2003). In semi-arid and arid ecosystems, surface lateral flow also occurs when rainfall intensity exceeds the infiltration capacity of dry soils (Kim and Eltahir, 2004). The universality and significance of lateral water flow in terrestrial ecosystems

HESSD
10, 12537–12571, 2013

suggests that it shouldn't have been overlooked by ecosystem and carbon cycle models. A better understanding of how lateral water flow and its spatial connectivity may affect water and carbon dynamics is therefore important for accurate quantification of terrestrial water and carbon budgets as well as sustainable management of water and forest resources (e.g., Wang et al., 2011).

The overall objective of this study is to investigate how consideration of water routing in a process-based, hydroecological model affects simulated water and carbon dynamics in terrestrial ecosystems. Toward this end, we rasterized an existing hydroecological model of hierarchical model framework designed to simulate integrated water, carbon and nutrient dynamics at watershed and regional scales. The rasterization aimed to (i) remove the model's hierarchical structure so that all hydrological and ecological processes would be simulated at the individual cell level; and (ii) add a new control interface so that the water routing algorithm built into the model could be switched on or off. These modifications allowed us to keep all model parameters and their parameterization identical between two predesigned simulations: one with and another without water routing. In turn, this helped reduce the uncertainty of model-based comparisons that can result from differences in model structure, parameters, and parameterization – as commonly encountered in model-based inter-comparison studies. The simulated soil water table depth and saturation deficit, evaporation, transpiration, evapotranspiration, forest productivity, and soil respiration from the two contrasting simulations were compared. Findings gained from these comparisons provide insights into the future development of ecosystem and carbon cycle models for terrestrial ecosystems.

2 Material and data

2.1 Study area

The Biscuit watershed in the Catskill Mountain Region of New York State (Fig. 1) was selected as the study region because (i) long-term historical stream flow observations

HESSD
10, 12537–12571, 2013

from one USGS gauge station (01434025) for this watershed are available to calibrate and evaluate model simulations; (ii) this watershed is forested and thus well suited for investigating the linkages between ecological and hydrological processes; (iii) there are no human-related land use activities; and (iv) the watershed has spatially variable terrain with elevation varying from 270 to 1270 m, providing a natural hydro-ecological laboratory to examine the effects of lateral water flow and its spatial connectivity on water, carbon and vegetation dynamics in terrestrial ecosystems.

2.2 Rasterizing the regional hydro-ecological simulation systems

The Regional Hydro-Ecological Simulation Systems (RHESSys) (Tague and Band, 2004) is a process-based hydro-ecological model designed for simulating integrated water, carbon and nutrient dynamics as well as vegetation growth at watershed and regional scales. Although RHESSys is capable of being run in fully distributed mode, its hierarchical model framework requires that some initial-state variables associated with the spatial hierarchy of basins, hillslopes and zones be arranged as per a prescribed template. In this study, we further rasterized RHESSys in an attempt to remove the model's hierarchical structure. The rasterized RHESSys (R-RHESSys) adopted almost all features of its predecessor except for (i) the exclusion of the hierarchical model framework of RHESSys, and (ii) the modification of the user-interface for controlling model simulation. The exclusion of the hierarchical structure in R-RHESSys caused the basin, hillslope and zone hierarchical structures existing in RHESSys to exist no longer. As a result, arrangement of some initial-state variables according to the prescribed template (i.e., the World file in RHESSys) is no longer needed. In addition, R-RHESSys excluded the TOPMODEL (Beven and Kirkby, 1979) embedded in its predecessor and adopted the explicit water routing algorithm (Wigmosta et al., 1994) for simulating surface and subsurface lateral flow as well as movement of solutes through space. The water routing algorithm in R-RHESSys can be switched on or off and thus provides users two ways (i.e., with vs. without water routing) to quantify carbon, wa-

HESSD
10, 12537–12571, 2013

ter, and nutrient dynamics in terrestrial ecosystems. As in its predecessor, surface and subsurface lateral flow for stream-type patches are channelized in R-RHESSys.

Because specific algorithms for carbon, water and nutrient dynamics are maintained mostly as in Tague and Band (2004), we herein briefly introduce the calculation of subsurface and surface flow that is slightly modified for reference. In R-RHESSys, the saturated subsurface flow ($SF_{a\to b}$) (m day^{-1}) from patch a to b is calculated as follows:

$$SF_{a\to b} = \begin{cases} \delta \times \gamma \times (e^{-s/m} - e^{-s_{max}/m}) & s \geq 0 \\ \delta \times \gamma \times (e^{-s/(3.5\,m)} - e^{-s_{max}/m}) & s < 0 \end{cases} \quad (1)$$

where, S (m) is saturation deficit in patch a; m (dimensionless) is the decay rate of soil hydraulic conductivity with depth in patch a; s_{max} (m) is the water equivalent of soil depth; δ (dimensionless) is the empirical sensitivity parameter with a value of 1.2 when water routing is considered and a value of 0.16 when water routing is ignored; γ (m day^{-1}) is the percent of subsurface flow going from patch a to patch b. It is expressed as:

$$\gamma = K_{sat0} \times \tan\beta_{a\to b} \times W_{a\to b} \quad (2)$$

where K_{sat0} (m day^{-1}) is saturated hydraulic conductivity at the surface; β (degree) is the local slope from patch a to patch b; and W (dimensionless) is the flow width from patch a to patch b. The flow widths are assumed to be 0.5 times the grid size for cardinal directions and 0.354 times the grid size for diagonal directions (Quinn et al., 1991; Tague and Band, 2004).

The saturation overland flow (RF_a) for patch a is expressed as follows:

$$RF_a = \max(RS + U_{satS} - S, 0.0) \quad (3)$$

where RS (m) is soil water storage in the root zone layer; and U_{satS} (m) is soil water storage in the un-saturated soil layer.

HESSD
10, 12537–12571, 2013

Unlike RHESSys that first simulates surface and subsurface flow for all patches and then route simulated surface and subsurface flow at a patch to its neighbors for update, R-RHESSys routes surface and subsurface flow in a patch to its neighbors immediately as soon as they are simulated in the patch. In practice, when comparing simulated flow to observed data at a gauge station, we assumed that the simulated subsurface and surface flow in all patches inside a watershed will flow out of the gauge station within a day when water routing is ignored. When water routing is considered, the calculated subsurface (or base) and saturation overland (or return) flow for stream-type patches are summed to compare to observed data.

2.3 Meteorological data

Time-series daily maximum and minimum temperature (°C) as well as total precipitation (mm) are required to run R-RHESSys. Because there is no weather station located in the Biscuit watershed, our climate data for the period 1961–2008, a period having as long as possible available climate records and preselected for model spin-up simulation, were derived from ten Cooperative Observer Program stations (COOP) (Fig. 1). Specifically, daily climate data for each day in each year for the watershed were estimated using the ordinary-Kriging interpolation approach (Goovaerts, 1998). Before interpolation, daily records of temperatures that exceeded the long-term (1961–2008) mean of all available records from that station by four standard deviations or greater were manually removed on a case-by-case basis (e.g., Tang and Arnone, 2013). In addition, local lapse rates of $-0.0085\,^{\circ}\mathrm{C\,m^{-1}}$ for daily maximum temperature, $-0.0054\,^{\circ}\mathrm{C\,m^{-1}}$ for daily minimum temperature, and $0.0014\,\mathrm{mm\,m^{-1}}$ for daily precipitation were used to adjust temperature and orographic precipitation changes along the elevation gradient in the study sites. Figure S1 in Supplement show examples of interpolated daily maximum and minimum temperature as well as precipitation for the Biscuit watershed in July 1994.

HESSD
10, 12537–12571, 2013

2.4 Land cover and soil data

The land cover data used to define vegetation types for the Biscuit watershed were based on the 1992 National Land Cover Data (NLCD 1992; http://www.epa.gov/mrlc/nlcd.html). The NLCD 1992 were derived from Landsat Thematic Mapper satellite data at 30 m spatial resolution and classified land covers into 21 types for the United States (Vogelmann et al., 1998a,b). For the Biscuit watershed, only three types exist in NLCD 1992: evergreen, deciduous and mixed forests. Our soil texture data at 30 m spatial resolution were derived from the digital Soil Survey Geographic Database (http://soils.usda.gov/). We classified soil in the Biscuit watershed into four types: sandy loam, loamy skeleton, silt loam and rocky (Fig. S1d, Supplement). Soil texture related parameters and their parameterization are in Table 1.

2.5 Modeling protocol, model calibration and evaluation

Our initial simulations using time-series daily climate data for the period 1961–2008 suggested that soil water table depth, leaf area index (LAI) and forest productivity tended to reach the equilibrium state after 50 simulation-years. In contrast, soil carbon took more than 200 simulation-years to reach the equilibrium state (Fig. S2, Supplement). In order to have vegetation and soil carbon reach equilibrium state with long-term local climate, we spun up R-RHESSys for 240 yr repeatedly using 48 yr (1961–2008) daily-step meteorological data. After spin-up simulations, we continued to run R-RHESSys for an additional 48 yr using data from 1961 to 2008. We calibrated R-RHESSys for the period 1992–1993 and evaluated it for the period 1994–1995. The period 1992–1995 was selected because observed climate records in this period from 10 COOP stations were more consistent than during other periods. This can minimize the effects of the quality of atmospheric forcing data on simulated water and carbon dynamics.

To investigate how consideration of water routing affects simulated water and carbon dynamics in the forested watershed, simulations with and without water routing

HESSD
10, 12537–12571, 2013

were performed. Correspondingly, model calibration and evaluation for each of the two pre-specified periods were performed for the two contrasting simulations, respectively. Monthly average daily values of major hydro-ecological variables in July 1994 from the two simulations were compared. The July 1994 was selected because temperature in July is generally higher than in other months and thus the effects of consideration of water routing on simulated water and carbon dynamics as well as vegetation growth were assumed to be more detectable.

3 Results

3.1 Calibration and evaluation of simulated stream flow and base flow

Figure 2 shows the time-series of simulated daily stream and base flow for Brook River in the Biscuit watershed for the calibration period 1992–1993 and for the evaluation period 1994–1995. For the calibration period, the calculated Nash–Sutcliffe coefficients (NS; Nash and Sutcliffe, 1970) is 0.59 for stream flow (Fig. 2a) and 0.68 for base flow (Fig. 2b) under the simulation that neglected water routing. In contrast, the calculated NS is 0.59 for stream flow (Fig. 2c) and 0.59 for base flow (Fig. 2d) for the simulation that considered water routing. For the evaluation period, the calculated NS is over 0.63 for both stream and base flow regardless of whether or not water routing was considered (Fig. 2a–d). In addition, the simulated average daily stream flow for the evaluation period 1994–1995 approximated each other between the two simulations (2.55 vs. 2.50 mm day^{-1}). Difference in average daily stream flow between model simulations and observation was less than 1.25 % under both simulations. These statistics (Table S1, Supplement) suggested that R-RHESSys was able to accurately simulate daily stream and base flow regardless of whether water routing was considered.

HESSD
10, 12537–12571, 2013

3.2 Comparison of simulated soil water table depth and saturation deficit

When water routing was considered, the simulated depth to the soil water table ranged from 0 to 2.28 m among cells and averaged 1.04 m for the entire watershed. In contrast, when water routing was ignored, the simulated depth ranged from 0 to 1.42 m among cells, and averaged 0.70 m for the entire watershed. In other words, the simulated water table depth was spatially more variable when water routing was simulated as indicated by the calculated standard deviations for soil water table depth among cells (Table 2 and Fig. 3a vs. b). A similar situation applied to the simulated saturation deficit, which had a wider range from 0 to 1.25 m under simulation with water routing but a narrower range from 0 to 0.63 m under simulation without water routing (Table 2). The simulated saturation deficit also was spatially more variable under simulation with water routing compared to that without water routing (Fig. 3d vs. e), as indicated by the standard deviations for saturation deficit among cells (Table 2). Further comparison suggested that water table depth and saturation deficit were about 0.5 m (for water table) and 0.3 m (for saturation deficit) greater in the hills or ridges of the Biscuit watershed when water routing was considered. In the valleys or flat areas, however, there are regions where the simulated water table depth and saturation deficit was smaller when water routing was considered compared to the simulation ignoring water routing (Fig. 3c and f). Spatially, deeper water table depth and higher saturation deficit were simulated to occur mostly at upslope areas (Fig. 3a and d) when water routing was considered. This situation, however, did not always apply to simulations without water routing, under which water table depth and saturation deficit were found to be greater at greater slopes (Fig. 3b and e).

3.3 Comparison of simulated evaporation, transpiration, and evapotranspiration

Compared to the simulation ignoring water routing, the simulated monthly average daily evaporation, transpiration, and actual evapotranspiration (ET) with water routing have

HESSD
10, 12537–12571, 2013

a wider range among cells. For example, monthly average daily evaporation was simulated to vary from 0.24 to 1.97 mm day^{-1} among cells under simulation with water routing. In contrast, evaporation has a narrower range from 0.49 to 1.00 mm day^{-1} under the simulation without water routing (Table 2). Nevertheless, when averaged for the entire watershed, monthly average daily evaporation, plant transpiration and ET approximated (difference < 0.02 %) each other between the two simulations (Table 2). In addition, regardless of the actual magnitudes of simulated water fluxes, the spatial patterns of evaporation, transpiration and ET were modeled to be extremely similar between the two simulations although extreme high and low values of evaporation, transpiration and ET were simulated to occur under the simulation with water routing (Figs. S3, Supplement, and 4). Spatially, the effects of consideration of water routing on simulated evaporation, transpiration and ET can be either positive or negative compared to the simulation neglecting water routing (Fig. S3, Supplement).

3.4 Comparison of simulated forest net primary productivity (NPP)

At the individual cell level, the simulated monthly average daily NPP in July 1994 when ignoring water routing ranged from 2.37 to 6.2 g C m^{-2}, narrower than results from the simulation considering water routing which ranged from 0.03 to 6.2 g C m^{-2} among cells. In addition, although the pattern of simulated NPP was extremely similar between the two simulations (Fig. 5a and b), the simulated monthly average daily NPP among cells was spatially more variable when water routing was considered, as suggested by the calculated standard deviations for NPP among cells (Table 2). When averaged for the entire watershed, however, the simulated monthly average daily NPP were almost identical (3.86 vs. 3.85 g C m^{-2}) between the two simulations (Table 2). In addition, the simulated maximum NPP between the two simulations was identical (6.2 g C m^{-2}), although there were regions where the simulated NPP values were distinctly lower (< 2.37 g C m^{-2}) under the simulation considered than that ignored water routing (> 2.37 g C m^{-2}). Overall, it seemed that the simulation neglecting water routing had a tendency to overestimate forest NPP in some areas of the watershed (Fig. 5c).

HESSD
10, 12537–12571, 2013

3.5 Comparison of simulated soil autotrophic and heterotrophic respiration

Simulated monthly average daily soil autotrophic respiration (RA) in July 1994 ranged from 0.0 to 0.70 $g C m^{-2}$ under the simulation with water routing. This range was slightly wider than that from the simulation without water routing, which ranged from 0.23 to 0.70 $g C m^{-2}$ (Table 2). When averaged for the entire watershed, however, monthly average daily soil RA approximated each other between the two simulations (0.48 vs. 0.47 $g C m^{-2}$; Table 2). In addition, the spatial pattern of simulated soil RA across the watershed was extremely similar between the two simulations (Fig. 6a and b) although there were patches where simulated soil RA was much lower when water routing was considered (Fig. 6c). Overall, neglect of water routing has the potential to cause R-RHESSys to overestimate soil RA while such overestimates were not significant in most areas of the watershed (Fig. 6c). Similarly, the simulated soil heterotrophic respiration (RH) had a wider range from 0.01 to 0.7 $g C m^{-2}$ under simulation with water routing and a narrower range from 0.51 to 0.7 $g C m^{-2}$ under the simulation without water routing (Table 2). Nevertheless, the spatial patterns of simulated soil RH were extremely similar between the two simulations (Fig. 6d and e). Besides, when averaged for the entire watershed, monthly average daily soil RH approximated each other (0.48 vs. 0.47 $g C m^{-2}$) between the two simulations. Differing from soil RA, the effects of water routing on soil RH can be either positive or negative when compared to the simulation without water routing (Fig. 6f). The difference in simulated soil RH between the two simulations ranged from −0.69 to 0.11 $g C m^{-2}$ across cells.

4 Discussion

4.1 Performance and accuracy of R-RHESSys

Our model evaluation against observed stream flow and derived base flow from the USGS gauge station indicated that R-RHESSys is able to accurately simulate river

HESSD
10, 12537–12571, 2013

flow at watershed scales, largely because all algorithms for water, carbon and nutrient dynamics as well as model parameters are maintained as in RHESSys, which itself has been applied and evaluated in a number of studies (e.g., Christensen et al., 2008; Hwang et al., 2012; Tague and Band, 2001). In addition, the simulated ecological variables – such as LAI and forest NPP – all fall within the ranges of corresponding field observations. For example, the modeled LAI in the growing season (May to September) averaged 3.3 $m^2 m^{-2}$ for the entire watershed and ranged from 1.32 to 4.2 $m^2 m^{-2}$ across grid cells, agreeing well with observed and modeled values that range from 2.90 to 4.5 $m^2 m^{-2}$ in mixed oak-hickory forest (Scurlock et al., 2001; Tang and Beckage, 2010), a dominant forest type in the study watershed. Our modeled annual forest NPP averaged 509 $g C m^{-2} yr^{-1}$, falling within the range of 391 to 574 $g C m^{-2} yr^{-1}$ of field observations in oak-hickories (e.g., Pan et al., 2006; Tang et al., 2010). Nevertheless, we acknowledged that the lack of spatially distributed field measurements – such as observed soil moisture, water table depth, and forest NPP – hinders us from further evaluating the patterns of simulated major ecological and hydrological variables across the watershed. Such limitations in the model's evaluation are encountered commonly in many other distributed-model-based studies (Brooks et al., 2007) and need improvement in the future.

4.2 Effects of water routing on soil water table depth and saturation deficit

Lateral water flow and associated water redistribution across the landscape considerably influence the hydrologic response in terrestrial ecosystems, including movement and storage of water in the soil (Guntner and Bronstert, 2004; Thompson and Moore, 1996). Some studies (e.g., Kim and Eltahir, 2004) indicated that topography drives lateral transport of water downslope, and water converges into concave areas or valleys through surface or subsurface runoff. As a result, water table depth tends to be significantly shallower in the valleys compared to the hills. However, this contrasting pattern does not occur in simulations that ignored water routing, in which the simulated water table depth and saturation deficit approximated each other between valleys and

HESSD
10, 12537–12571, 2013

hills/ridges of the watershed (Fig. 3b and e). In other words, the simulated water table depth and saturation deficit with water routing captured better our preconception of their spatial patterns across the Biscuit watershed. A similar study in a humid watershed (Hotta et al., 2010) indicated that lateral flow and local infiltration descending from hillslopes often causes lower elevation sites to have a higher water table level and higher elevation sites to have a lower water table level.

Additionally, a similar model-based comparison study supported our findings. Sonnentag et al. (2008) compared simulated water table depth between simulations with and without considering lateral water flow in a peatland. They found that the magnitude of simulated water table depth without water routing was considerably underestimated because lateral subsurface flow moves water toward the margins of the peat body. The neglect of lateral flow resulted in the simulated water table at or very close to the ground surface, which explains why the simulated water table depth was much greater under simulation ignoring water routing (Table 2). Furthermore, Moore and Thompson (1996) found that the combination of slope curvature, microtopography and resulting water movement can produce significant variability in water table depth across the landscape. This explains why the calculated standard deviation of water table depth among cells almost doubled (0.35) under simulation considering compared to that (0.19) ignoring water routing (Table 2).

Similar to water table depth, saturation deficit under simulation with water routing showed a distinct pattern in the watershed: smaller in the valleys and greater in the hills or ridges of the watershed, which agreed better with findings from previous studies. Hopp et al. (2009) found that a relatively high saturation in the soil profile occur in the swale and drier zones often occur upslope and on the side ridges of hillslopes when water routing and topography were both considered in the model simulation. Crave and Gascuel-Odoux (1997) indicated that the steeper upslope parts of a watershed will be drained laterally more rapidly than the gentler downslope parts, resulting in drier slopes at the catchment scale. These patterns were captured by simulation with water routing (Fig. 3d) while not always captured by simulation without water routing (Fig. 3e). In

HESSD
10, 12537–12571, 2013

addition, most previous studies indicated that the upslope contributing area, as incorporated into the TOPMODEL (Beven and Kirkby, 1979), is probably the major topographic influence on soil moisture distribution (e.g., Hotta et al., 2010; Thompson and Moore, 1996). This relationship also was captured better by simulation considering water routing as suggested by the strength of the linear relationship of simulated saturation deficit to calculated topographic wetness index (Fig. 7a vs. b) between the two simulations.

4.3 Effects of water routing on water fluxes from land to the atmosphere

Slope, aspect and surrounding topography control incident direct solar radiation, and lower-elevation regions in mountainous watersheds have more incoming longwave radiation from the surrounding landscapes plus temperature decreases as elevation increases. The highest ET values often occur in valleys, and the lowest ET in north-facing, high elevation areas (Bertoldi et al., 2006; Christensen et al., 2008), which explains why the modeled spatial patterns of ET and transpiration in the watershed were higher in low elevations and valleys and lower in high elevations under the two simulations (Fig. S3, Supplement). Water routing is a major determinant of soil water table and moisture distribution, however, both of which play important roles in modulating water fluxes from land to the atmosphere. For example, Salvucci and Entekhabi (1995) indicated that deeper water table typically indicates drier areas where evaporation is often suppressed. It is why evaporation under simulation considering water routing was lower in most hills and ridges of the watershed compared to simulation ignoring water routing (Fig. S3c, Supplement). Such difference was not noticeable, however, when averaged for the entire watershed. An earlier model-based simulation study (Sonnentag et al., 2008) also suggested that neglecting shallower lateral flow and the resulting underestimation of soil water table depth have a tendency to overestimate evaporation because of increased soil wetness. Because forest productivity is modeled to be similar in most areas between the two simulations and because transpiration accounts for two-thirds of total ET plus water is not limited, simulated transpiration and ET were ex-

HESSD
10, 12537–12571, 2013

tremely similar in most areas of the watershed between the two simulations, although significant differences occurred in some areas (Fig. S3f and i, Supplement).

4.4 Effects of water routing on vegetation productivity

Changes in soil moisture condition affect canopy photosynthesis and forest productivity. Hwang et al. (2012) found that soil moisture content has profound effects on plant growth in forested watersheds. Svoray and Karnieli (2011) indicated that plant productivity is strongly correlated with water redistribution processes. Plants in the lower physiographic units (e.g., the footslope, the channel) should respond well to improved water and soil conditions and, therefore, should be more productive. In contrast, the interfluve, shoulder, and backslope areas often had lower vegetative greenness values because of poor water availability. In this study, the effects of differences in simulated soil moisture condition on forest productivity were not very noticeable between the two simulations, largely because incoming solar radiation and temperature are major determinants of forest productivity and these radiative forcings were identical between the two simulations. Thus, it is not surprising that the simulated pattern of forest NPP was extremely similar in most areas of the watershed between the two simulations. Nevertheless, because changes in soil moisture can affect forest productivity and because the saturation deficit was simulated to be greater under the simulation with water routing, simulated forest NPP was significantly lower in some areas of the watershed when water routing was considered. In fact, forest NPP was significantly and negatively correlated with saturation deficit in our simulation (Fig. 8a) because the deterioration of soil moisture condition can limit vegetation growth (e.g., Urgeghe et al., 2010).

4.5 Effects of water routing on soil respiration

Local topography can generate considerable spatial variability in soil temperature, incoming solar radiation, and soil water content (Running et al., 1987; Kang et al., 2004). Although each of these factors differentially affects soil respiration, soil temperature

HESSD
10, 12537–12571, 2013

plays a major role in soil respiration. Kang et al. (2004) found that about 75 % of seasonal variations in soil respiration can be explained by variation in soil temperature. Because soil temperature is simulated to be the same between the two simulations, this greatly contributed to (i) the similarity of the spatial pattern of simulated soil RA and RH (Fig. 6), and (ii) the proximity of daily respiration averaged for the entire watershed (Table 2). Indeed, the calculation of root RA in R-RHESS is mainly treated as a function of soil temperature, following Ryan et al. (1991). Because saturation deficit was higher when water routing was considered, and because soil water deficit limits the production of root, the consequent soil RA is thus slightly smaller under the simulation considering water routing (Fig. 6a–c), although the difference is small (< 2 %) with the exception of a few cells, in which the difference was as high as 40 % (Fig. 6c). Linear regression suggested that soil RA is negatively and significantly correlated with saturation deficit (Fig. 8b)

Although soil temperature plays a dominant role in regulating soil RH, changes in soil water content due to lateral flow and connectivity affect litter production and soil microbial activity, which in turn affect soil RH. Riveros-Iregui et al. (2011) indicated that the growing season soil CO_2 efflux is known to vary laterally by as much as seven-fold within small subalpine watersheds in the northern Rocky Mountains, and the variability was strongly related to the landscape-imposed redistribution of soil water. Because soil RH in R-RHESSys is treated as a function of soil moisture following Parton et al. (1996), this explains that the simulated soil RH is spatially more variable (higher standard deviation) among cells when water routing is considered (Table 2). In a semiarid subalpine watershed, Riveros-Iregui and McGlynn (2009) observed that the highest soil CO_2 efflux rates often occur in areas with persistently high soil moisture, whereas lower soil CO_2 efflux rates are on forested uplands in subalpine watersheds. Such patterns, however, was not simulated to occur in our humid watershed under the two simulations. Soil RH was generally simulated to be low in areas of deeper slopes (Figs. 1 and 6) because forest NPP and litter production were low in these areas. Compared to soil RA, differences in simulated soil RH between the two simulations were spatially more

HESSD
10, 12537–12571, 2013

variable largely due to combined effects of soil temperature, moisture and litter inputs on RH. Overall, soil RH was negatively correlated to the saturation deficit in our simulation, suggesting that neglect of water routing has potential to cause the model to overestimate soil RH (Fig. 8c).

5 Conclusions

Based on R-RHESSys and by keeping all model parameters and their parameterizations identical, this model-based comparison study indicated that:

i. R-RHESSys is able to correctly simulate stream and base flow for Brook River in the study watershed regardless of whether water routing is considered in the model simulation. When water routing is considered, however, it captures better our preconception of the spatial patterns of water table depth and saturation deficit. In contrast, when water routing is neglected, the simulation has a tendency to underestimate water table depth and saturation deficit. The simulated patterns of water table depth and saturation deficit differ from our preconception of the two quantities across the landscape.

ii. Difference in simulated water table depth and saturation deficit between simulations with and without water routing affects subsequent water fluxes from land to the atmosphere. At the individual cell level, simulated evaporation, transpiration and ET are spatially more heterogeneous across the landscape when water routing is considered. Although differences in simulated evaporation, plant transpiration and ET can be significant at the individual cell level between the two simulations, differences in these water fluxes are not significant when averaged for the entire watershed.

iii. Forest productivity is generally simulated to be smaller and spatially more variable under simulation with water routing due to higher and more variable saturation

HESSD
10, 12537–12571, 2013

deficit. Lower forest productivity and root production caused simulated soil RA to be slightly lower when water routing is considered. In contrast, simulated soil RH with water routing can be either greater or smaller than that without water routing due to the combined effects of soil moisture, temperature and litter inputs. When averaged for the entire watershed, however, differences in modeled forest productivity and soil respiration were insignificant between the two simulations.

Overall, this study indicated that lateral water flow exerts a strong control on the spatial pattern and variability of water table depth and saturation deficit (e.g., Mahmood and Vivoni, 2011). Although the simulated water fluxes from land to the atmosphere, forest productivity, and soil respiration were extremely similar when averaged for the entire watershed, simulation without water routing has the potential to overestimate forest productivity, evaporation, and soil respiration. Since the spatial pattern of soil moisture is fundamental to spatially distributed modeling of eco-hydrological processes (e.g., Chamran et al., 2002; Hebrard et al., 2006), ecosystem and carbon cycle models, therefore, need to explicitly represent water routing because simulation with water routing better captures the patterns of water table depth and saturation deficit across landscapes.

Supplementary material related to this article is available online at http://www.hydrol-earth-syst-sci-discuss.net/10/12537/2013/hessd-10-12537-2013-supplement.pdf.

Acknowledgement. The authors thank the New York City Department of Environmental Protection which provided funding for the research that led to this manuscript. This project also was supported by the NSF EPSCoR grant (NSF Cooperative 479 Agreement EPS-480 0814372) for Nevada.

References

Asbjornsen, H., Goldsmith, G. R., Alvarado-Barrientos, M. S., Rebel, K., Van Osch, F. P., Rietkerk, M., Chen, J., Gotsch, S., Tobon, C., Geissert, D. R., Gomez-Tagle, A., Vache, K., and Dawson, T. E.: Ecohydrological advances and applications in plant–water relations research: a review, J. Plant. Ecol., 4, 3–22, 2011.

Bertoldi, G., Rigon, R., and Over, T. H.: Impact of watershed geomorphic characteristics on the energy and water budgets, J. Hydrometeorol., 7, 389–403, 2006.

Beven, K. and Kirkby, M.: A physically-based variable contributing area model of basinhydrology, Hydrol. Sci. Bull., 24, 43–69, 1979.

Brooks, E. S., Boll, J., and McDanil, P. A.: Distributed and integrated response of a geographic information system-based hydrologic model in the eastern Palouse region, Idaho, Hydrol. Process., 21, 110–122, 2007.

Chamran, F., Gessler, P. E., and Chadwick, O. A.: Spatially explicit treatment of soil-water dynamics along a semiarid catena, Soil Sci. Soc. Am. J., 66, 1571–1583, 2002.

Chen, J. M., Chen, X., Ju, W., and Geng, X.: Distributed hydrological model for mapping evapotranspiration using remote sensing inputs, J. Hydrol., 305, 15–39, 2005.

Christensen, L., Tague, C. L., and Baron, J. S.: Spatial patterns of simulated transpiration response to climate variability in a snow dominated mountain ecosystem, Hydrol. Process., 22, 3576–3588, 2008.

Crave, A. and Gascuel-Odoux, C.: The influence of topography on time and space distribution of soil surface water content, Hydrol. Process., 11, 203–210, 1997.

Doten, C. O., Bowling, L. C., Lanini, J. S., Maurer, E. P., and Lettenmaier, D. P.: A spatially distributed model for the dynamic prediction of sediment erosion and transport in mountainous forested watersheds, Water Resour. Res., 42, W04417, doi:10.1029/2004WR003829, 2006.

Gérard-Marchant, P., Hively, W. D., and Steenhuis, T. S.: Distributed hydrological modelling of total dissolved phosphorus transport in an agricultural landscape, part I: distributed runoff generation, Hydrol. Earth Syst. Sci., 10, 245–261, doi:10.5194/hess-10-245-2006, 2006.

Goovaerts, P.: Ordinary cokriging revisited, Math. Geol., 30, 21–42, 1998.

Guntner, A. and Bronstert, A.: Representation of landscape variability and lateral redistribution processes for large-scale hydrological modelling in semi-arid areas, J. Hydrol., 297, 136–161, 2004.

HESSD
10, 12537–12571, 2013

Hebrard, O., Voltz, M., Andrieux, P., and Moussa, R.: Spatio-temporal distribution of soil surface moisture in a heterogeneously farmed Mediterranean catchment, J. Hydrol., 329, 110–121, 2006.

Hopp, L., Harman, C., Desilets, S. L. E., Graham, C. B., McDonnell, J. J., and Troch, P. A.: Hillslope hydrology under glass: confronting fundamental questions of soil-water-biota co-evolution at Biosphere 2, Hydrol. Earth Syst. Sci., 13, 2105–2118, doi:10.5194/hess-13-2105-2009, 2009.

Hotta, N., Tanaka, N., Sawano, S., Kuraji, K., Shiraki, K., and Suzuki, M.: Impact forest harvesting in steep, small watersheds, J. Hydrol., 385, 120–131, 2010.

Hwang, T., Band, L. E., Vose, J. M., and Tague, C.: Ecosystem processes at the watershed scale: hydrologic vegetation gradient as an indicator for lateral hydrologic connectivity of headwater catchments, Water Resour. Res., 48, W06514, doi:10.1029/2011WR011301, 2012.

Ivanov, V. Y., Bras, R. L., and Vivoni, E. R.: Vegetation-hydrology dynamics in complex terrain of semiarid areas: 2. Energy-water controls of vegetation spatiotemporal dynamics and topographic niches of favorability, Water Resour. Res., 44, W03430, doi:10.1029/2006WR005595, 2008.

Ju, W., Chen, J. M., Black, A. B., Barr, A. G., McCaughey, H., and Roulet, N. T.: Hydrological effects on carbon cycles of Canada's forests and wetlands, Tellus B, 58, 16–30, 2006.

Kang, S., Lee, D., and Kimball, J. S.: The effects of spatial aggregation of complex topography on hydro-ecological process simulations within a rugged forest landscape: development and application of a satellite-based topoclimatic model, Can. J. Forest Res., 34, 519–530, 2004.

Kim, Y. and Eltahir, E. A. B.: Role of topography in facilitating coexistence of trees and grasses within savannas, Water Resour. Res., 40, W07505, doi:10.1029/2003WR002578, 2004.

Lane, S. N., Reaney, S. M., and Heathwaite, A. L.: Representation of landscape hydrological connectivity using a topographically driven surface flow index, Water Resour. Res., 45, W08423, doi:10.1029/2008WR007336, 2009.

Mahmood, T. H. and Vivoni, E. R.: A climate-induced threshold in hydrologic response in a semiarid ponderosa pine hillslope, Water Resour. Res., 47, W09529, doi:10.1029/2011WR010384, 2011.

Moore, R. D. and Thompson, J. C.: Are water table variations in a shallow forest soil consistent with the TOPMODEL concept?, Water Resour. Res., 32, 663–669, 1996.

Nash, J. E. and Sutcliffe, J. V.: River flow forecasting through conceptual models Part I – A discussion of principles, J. Hydrol., 10, 282–290, 1970.
Pan, Y., Birdsey, R., Hom, J., McCullough, K., and Clark, K.: Improved estimates of net primary productivity from MODIS satellite data at regional and local scales, Ecol. Appl., 16, 125–132, 2006.
Parton, W. J., Mosier, A. R., Ojima, D. S., Valentine, D. W., Schimel, D. S., Weier, K., and Kulmala, A. E.: Generalized model for N_2 and N_2O production from nitrification and denitrification, Global Biogeochem. Cy., 10, 401–412, 1996.
Pockman, W. T. and Small, E. E.: The influence of spatial patterns of soil moisture on the grass and shrub responses to a summer rainstorm in a Chihuahuan Desert ecotone, Ecosystems, 13, 511–525, 2010.
Price, M. F., Gratzer, G., Duguma, L. A., Kohler, T., Maselli, D., and Romeo, R. (Eds.): Mountain Forests in a Changing World – Realizing Values, Addressing Challenges, FAO/MPS and SDC, Rome, 2011.
Quinn, P., Beven, K., Chevallier, P., and Planchon, O.: The prediction of hillslope flow paths for distributed hydrological modeling using digital terrain models, Hydrol. Process., 5, 59–79, 1991.
Ridolfi, L., D'Odorico, P., Porporato, A., and Rodriguez-Iturbe, I.: Stochastic soil moisture dynamics along a hillslope, J. Hydrol., 272, 264–275, 2003.
Riveros-Iregui, D. A. and McGlynn, B. L.: Landscape structure control on soil CO_2 efflux variability in complex terrain: scaling from point observations to watershed scale fluxes, J. Geophys. Res.-Biogeo., 114, G02010, doi:10.1029/2008JG000885, 2009.
Riveros-Iregui, D. A., McGlynn, B. L., Marshall, L. A., Welsch, D. L., Emanuel, R. E., and Epstein, H. E.: A watershed-scale assessment of a process soil CO_2 production and efflux model, Water Resour. Res., 47, W00J04, doi:10.1029/2010WR009941, 2011.
Running, S. W., Nemani, R. R., and Hungerford, R. D.: Extrapolation of synoptic meteorological data in mountainous terrain and its use for simulating forest evapotranspiration and photosynthesis, Can. J. Forest Res., 17, 472–483, 1987.
Ryan, M. G.: Effects of climate change on plant respiration, Ecol. Appl., 1, 157–167, 1991.
Salvucci, G. D. and Entekhabi, D.: Hillslope and climatic controls on hydrologic fluxes, Water Resour. Res., 31, 1725–1739, 1995.
Scurlock, J. M. O., Asner, G. P., and Gower, S. T.: Global leaf area index from field measurements, 1932–2000, data source: Oak Ridge National Laboratory Distributed Active Archive

HESSD
10, 12537–12571, 2013

Center, Oak Ridge, Tennessee, USA, available at: http://www.daac.ornl.gov (last access: 15 October 2013), 2001.
Singh, R., Jhorar, R. K., van Dam, J. C., and Feddes, R. A.: Distributed ecohydrological modelling to evaluate irrigation system performance in Sirsa district, India II: Impact of viable water management scenarios, J. Hydrol., 329, 714–723, 2006.
Smith, M. B., Koren, V., Reed, S., Zhang, Z., Zhang, Y., Moreda, F., Cui, Z., Naoki, M., Anderson, E. A., and Cosgrove, B. A.: The distributed model intercomparison project – Phase 2: Motivation and design of the Oklahoma experiments, J. Hydrol., 418–419, 3–16, 2012.
Smith, M. W., Bracken, L. J., and Cox, N. J.: Toward a dynamic representation of hydrological connectivity at the hillslope scale in semiarid areas, Water Resour. Res., 46, W12540, doi:10.1029/2009WR008496, 2010.
Sonnentag, O., Chen, J. M., Roulet, N. T., Ju, W., and Govind, A.: Spatially explicit simulation of peatland hydrology and carbon dioxide exchange: influence of mesoscale topography, J. Geophys. Res.-Biogeo., 113, G02005, doi:10.1029/2007JG000605, 2008.
Sponseller, R. A. and Fisher, S. G.: The influence of drainage networks on patterns of soil respiration in a desert catchment, Ecology, 89, 1089–1100, 2008.
Svoray, T. and Karnieli, A.: Rainfall, topography and primary production relationships in a semi-arid ecosystem, Ecohydrology, 4, 56–66, 2011.
Tague, C. L. and Band, L. E.: Evaluating explicit and implicit routing for watershed hydro-ecological models of forest hydrology at the small catchment scale, Hydrol. Process., 15, 1415–1439, 2001.
Tague, C. L. and Band, L. E.: RHESSys: regional hydro-ecologic simulation system – an objected-oriented approach to spatially distributed modeling of carbon, water and nutrient cycling, Earth Interact., 8, 1–42, 2004.
Tang, G. and Arnone III, J.: Trends in surface air temperature and temperature extremes in the Great Basin during the 20th century from ground-based observations, J. Geophys. Res.-Atmos., 118, 3579–3589, 2013.
Tang, G. and Beckage, B.: Projecting the distribution of forests in New England in response to climate change, Divers. Distrib., 16, 144–158, 2010.
Tang, G., Beckage, B., Smith, B., and Miller, P. A.: Estimating potential forest NPP, biomass and their climatic sensitivity in New England using a regional dynamic ecosystem model, Ecosphere, 1, 1–20, 2010.

HESSD
10, 12537–12571, 2013

Consideration of water routing captures better water and carbon patterns

G. Tang et al.

Thompson, J. C. and Moore, R. D.: Relations between topography and water table depth in a shallow forest soil, Hydrol. Process., 10, 1513–1525, 1996.
Urgeghe, A. M., Breshears, D. D., Martens, S. N., and Beeson, P. C.: Redistribution of runoff among vegetation patch types: on ecohydrological optimality of herbaceous capture of run-on, Rangeland, Ecol. Manage., 63, 497–504, 2010.
Vogelmann, J. E., Sohl, T., Campbell, P. V., and Shaw, D. M.: Regional land cover characterization using landsat thematic mapper data and ancillary data sources, Environ. Monit. Assess., 51, 415–428, 1998a.
Vogelmann, J. E., Sohl, T., and Howard, S. M.: Regional characterization of land cover using multiple sources of data, Photogramm. Eng. Rem. S., 64, 45–47, 1998b.
Wang, J. H., Yang, H., Li, L., Gourley, J. J., Sadiq, I. K., Yilmaz, K. K., Adler, R. F., Policelli, F. S., Habib, S., Irwn, D., Limaye, A. S., Korme, T., and Okello, L.: The coupled routing and excess storage (CREST) distributed hydrological model, Hydrol. Sci. J., 56, 84–98, 2011.
Wang, L., Koike, T., Yang, K., Jackson, T. J., Bindlish, R., and Yang, D.: Development of a distributed biosphere hydrological model and its evaluation with the Southern Great Plains Experiments (SGP97 and SGP99), J. Geophys. Res.-Atmos., 114, D08107, doi:10.1029/2008JD010800, 2009.
Wigmosta, M., Vail, L., and Lettenmaier, D.: Distributed hydrology–vegetation model for complex terrain, Water Resour. Res., 30, 1665–1679, 1994.

HESSD
10, 12537–12571, 2013

Consideration of water routing captures better water and carbon patterns

G. Tang et al.

Table 1. Major soil parameters and their parameterizations used in this study.

Variables	Unit	Soil texture			
		Sandy loam	Silt loam	Loamy skeleton	Rocky
K_{sat0}	m day^{-1}	89.05	48.62	48.36	109.56
m	DIM	0.09	0.12	0.13	0.09
Porosity	%	0.435	0.410	0.451	0.485
Porosity decay	DIM	4000	4000	4000	4000
Pore size index (PSI)	DIM (0–1)	0.204	0.189	0.186	0.228
PSI air entry	%	0.218	0.386	0.478	0.480
Soil depth	m	5.0	5.2	4.8	5.0
Active zone depth	m	10.0	10.0	10.0	10.0
Maximum energy capacity	°C	−10.0	−10.0	−10.	−10.0
Albedo	DIM	0.258	0.253	0.320	0.200
Sand	%	0.70	0.20	0.80	0.75
Clay	%	0.10	0.15	0.02	0.05
Silt	%	0.20	0.65	0.18	0.20

K_{sat0} is saturated hydraulic conductivity at the surface; m is the decay rate of hydraulic conductivity with depth.

HESSD
10, 12537–12571, 2013

Table 2. Comparison of simulated hydrological and ecological variables between simulations with and without water routing.

Variables	Water routing	Minimum	Maximum	Mean	STD
water table depth (m)	Yes	0.081	2.278	1.037	0.35
	No	0.005	1.424	0.698	0.19
saturation deficit (m)	Yes	0.039	1.027	0.476	0.15
	No	0.002	0.642	0.322	0.08
Evaporation (mm)	Yes	0.24	1.97	0.73	0.06
	No	0.49	1.00	0.73	0.05
Plant transpiration (mm)	Yes	0.06	2.19	1.12	0.12
	No	0.76	1.67	1.12	0.11
Evapotranspiration (mm)	Yes	0.34	2.72	1.85	0.17
	No	1.25	2.67	1.85	0.16
NPP ($g\,C\,m^{-2}\,day^{-1}$)	Yes	0.03	6.2	3.85	0.34
	No	2.37	6.2	3.86	0.22
RA ($g\,C\,m^{-2}\,day^{-1}$)	Yes	0.00	0.7	0.47	0.07
	No	0.23	0.7	0.48	0.07
RH ($g\,C\,m^{-2}\,day^{-1}$)	Yes	0.01	1.51	0.99	0.10
	No	0.51	1.49	1.00	0.08

HESSD
10, 12537–12571, 2013

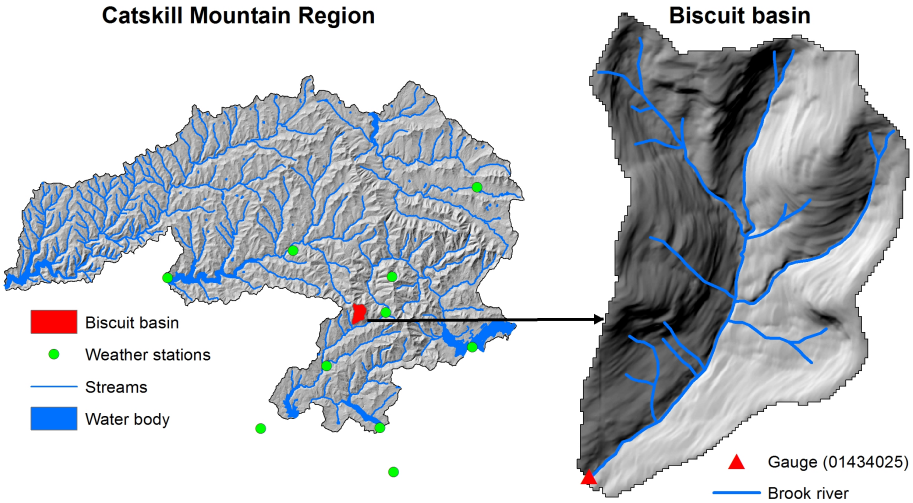

Fig. 1. The location of the Biscuit watershed (red area) and the United States Geological Survey gauge station within the Catskill Mountain region of New York State. The map on the left depicts the boundaries of the West of Hudson watershed and reservoirs of the New York City water supply system. The green points are ten Cooperative Observer Program weather stations used to derive meteorological data for the Biscuit watershed.

HESSD
10, 12537–12571, 2013

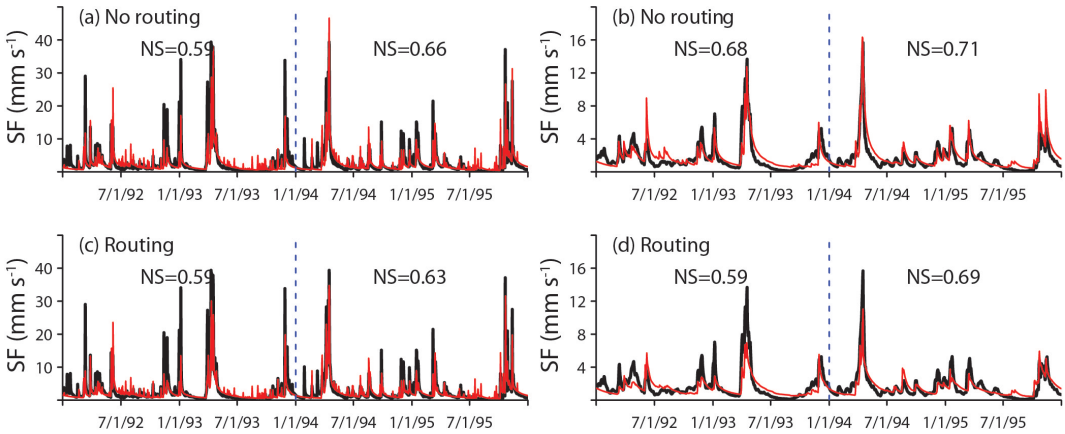

Fig. 2. Calibration (for the period 1 January 1992–31 December 1993) and evaluation (for the period 1 January 1994–31 December 1995) of R-RHESSys simualted daily stream flow (SF) and base flow (BF) (solid red line) against observed/derived data (solid black line). Simulations in **(a)** and **(b)** ignored while simulations in **(c)** and **(d)** considered water routing. NS is short for the Nash–Sutcliff coefficient. The blue dashed line represnts 1 January 1994.

HESSD
10, 12537–12571, 2013

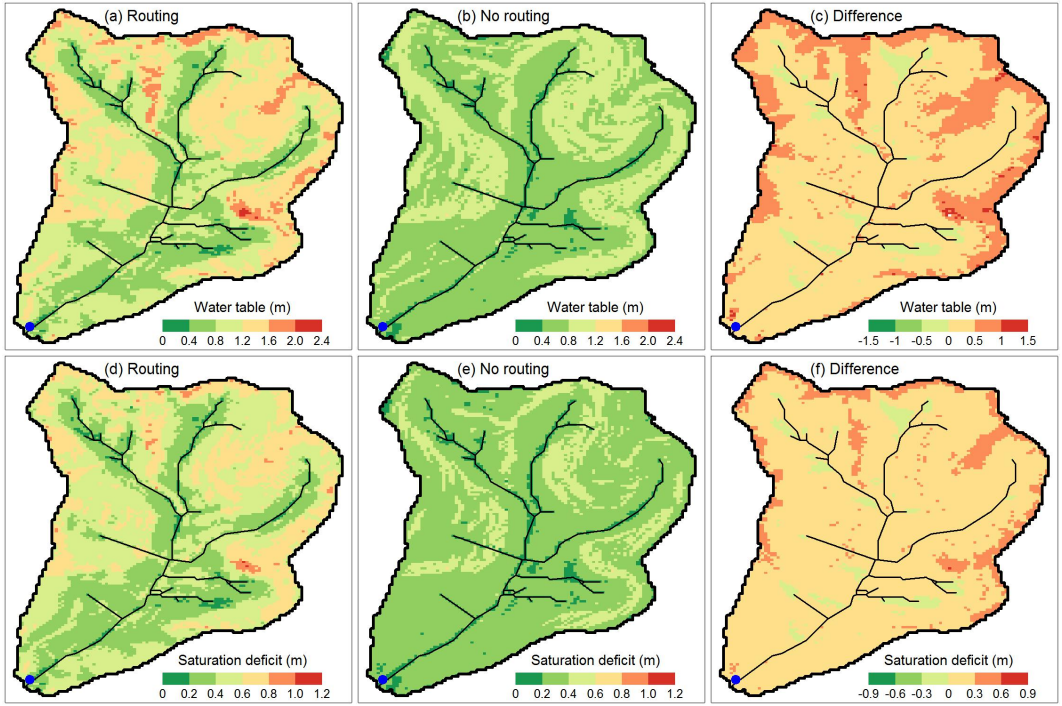

Fig. 3. Comparison of simulated monthly average daily soil water table depth and saturation deficit in July 1994 between the two simulations: **(a)** and **(d)** considering water routing while **(b)** and **(e)** ignoring water routing. **(c)** and **(f)** show differences in simulated soil water table depth and saturation deifict between the two simulations.

HESSD
10, 12537–12571, 2013

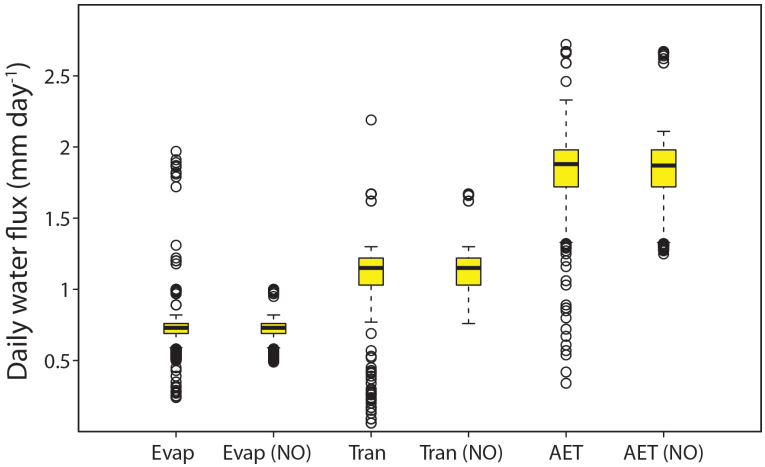

Fig. 4. Comparison of simulated monthly average daily evaporation (evap), transpiration (Tran), and actual evapotranspiration (AET) in July 1994 between the two simulations with and without (indicated by "NO") consideration of water routing.

HESSD
10, 12537–12571, 2013

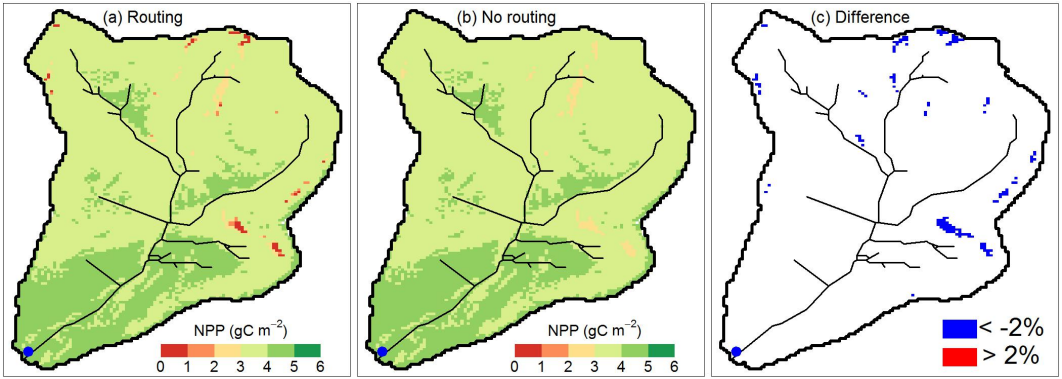

Fig. 5. Comparison of simulated monthly average daily net primary productivity (NPP) in July 1994 between the two simulations: **(a)** considering water routing and **(b)** ignoring water routing. **(c)** shows percentage difference between **(a)** and **(b)** divided by the result from simulation **(a)** considering water routing.

HESSD
10, 12537–12571, 2013

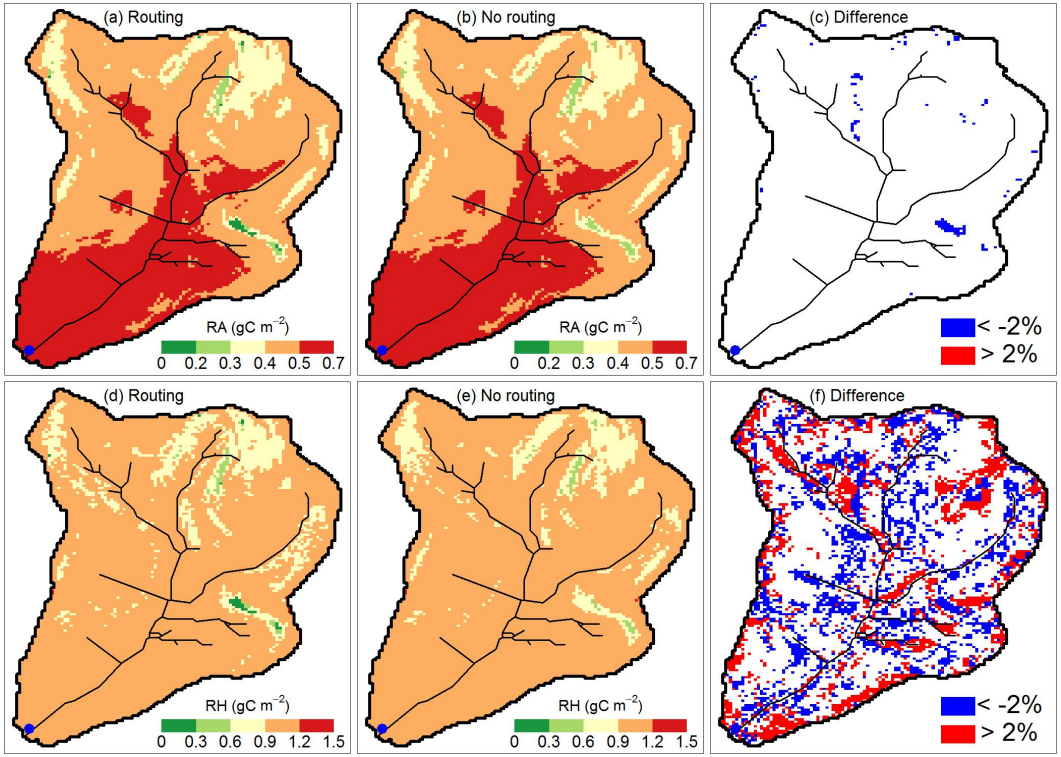

Fig. 6. Comparison of simulated monthly average daily soil autotrophic (RA) and heterotrophic respiration (RH) in July 1994 between the two simulations: **(a)** and **(d)** considering while **(b)** and **(e)** ignoring water routing. **(c)** and **(f)** show percentage differences between the two simulations divided by results from simulation considering water routing.

HESSD
10, 12537–12571, 2013

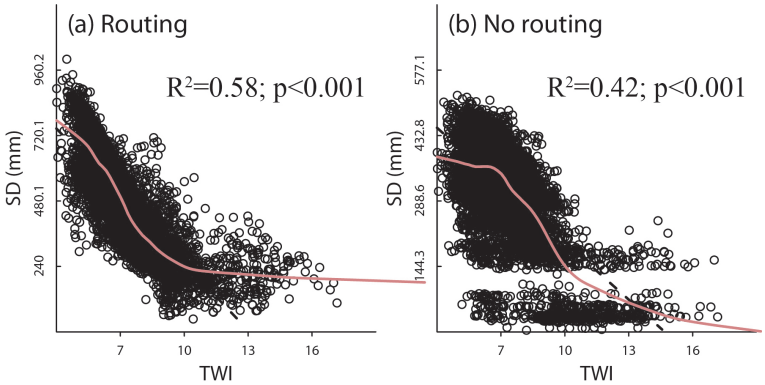

Fig. 7. Comparison of the relationships of simulated saturation deificit (SD) to topographic wetness index (TWI) across the watershed between the two simulations: **(a)** considering water routing and **(b)** ignoring water routing.

HESSD
10, 12537–12571, 2013

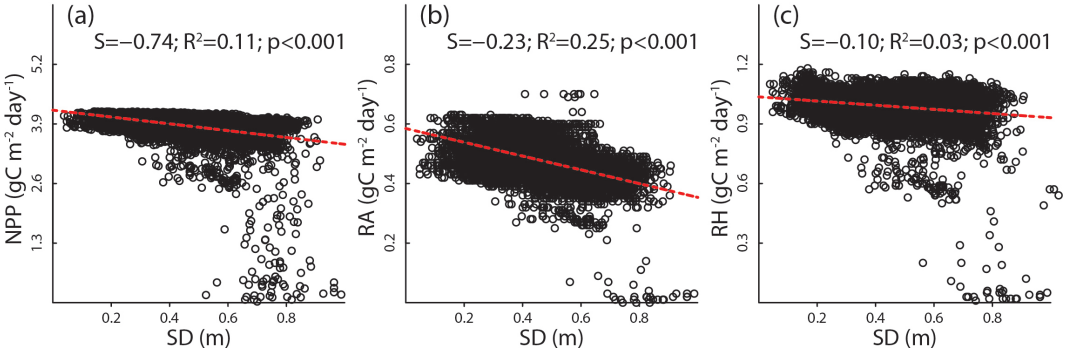

Fig. 8. The relationships of saturation deficit (SD) with net primary productivity (NPP), **(b)** soil autotrophic respiration (RA), and **(c)** soil heterotrophic respiration (RH). Data shown here are based on the simulation considering water routing.

HESSD
10, 12537–12571, 2013